ELSEVIER Computers and Electronics in Agriculture 15 (1996) 161–179

Computers and electronics in agriculture

Tracking of row structure in three crops using image analysis

J.A. Marchant

Silsoe Research Institute, Wrest Park, Silsoe, Bedford MK45 4HS, UK

Accepted 11 March 1996

Abstract

This paper is concerned with visual sensing for an autonomous crop protection robot, in particular the problem of finding guidance information from crop row structure. A robust method for finding crop rows in images has been presented in the author's previous work and is briefly re-introduced here. This is based on the Hough transform but, unlike previous methods, integrates information over a number of crop rows making the technique very tolerant to such problems as missing plants and weeds. Experiments are reported where the method is tested on three crops; cauliflowers, sugar beet, and widely spaced double rows of wheat. When compared with a human assessment of the row positions in images, typical errors were 18 mm of lateral offset and 1° of angle.

Keywords: Image analysis; Robotics; Control; Weeds; Row crops; Sugar beet; Cereals

1. Introduction

In recent decades, farming in the western world has come to rely more and more on chemical crop protection. At present approximately 23,000 tonnes of chemicals are used annually in the UK at a cost of about £400 million. Lately this heavy use of chemicals has provoked demands from consumers and environmentalists for reduction. A potential way of meeting these demands is the use of precision techniques for various types of agricultural operations, in particular the application of chemicals of all kinds so that they are placed where they will have an optimal effect with minimum quantity.

The work described here is part of research to develop the technology for controlling an autonomous vehicle for precision crop protection. The aim is to sense targets on-line and to work on a plant scale, that is with an accuracy of a few centimetres relative to the plants themselves. This is in contrast to existing work on spatially selective operations (e.g. Stafford and Ambler, 1994) where field maps are built up from prior knowledge and treatment areas are on a scale of a metre or so based on an absolute coordinate system. The vehicle is fitted with various sensors, including image analysis, which

PII S0168-1699(96)00014-2

Fig. 1. Autonomous vehicle in a field of cauliflowers.

are used together to derive guidance information. A description is contained in Hague and Tillett (1996) and the vehicle is shown in Fig. 1. Image analysis is also used for differentiating between plants, weeds, and soil (Brivot and Marchant, 1996). The present work is confined to situations where plants are established in rows and this paper reports some results using an algorithm to track rows in images of three crops: cauliflowers, sugar beet, and cereals grown in widely spaced rows.

2. Previous work

The problem of finding direction from planting structure has received a considerable amount of attention. Two basic situations have been considered: that where harvesting or mowing changes the scene to one side of a line (Gerrish and Stockman, 1985; Fehr and Gerrish, 1989; Brown et al., 1990; Derras et al., 1991), and the other where plants are grown in rows producing a natural set of lines in the image (Gerrish and Stockman, 1985; Reid and Searcy, 1986; Brandon et al., 1989; Schoenfisch and Billingsley, 1993). In the former situation some sort of global difference between the two regions, such as texture or average grey level, is used to find a boundary and then a line fitting method, such as regression, is used to find the line position and direction. As the situation is somewhat different from our row crop one it will not be considered further here.

Most authors have recognised that real images are likely to suffer from problems such as incomplete row lines and poor contrast between plants and background. Brandon et al. (1989) use near infra-red wavelengths to enhance contrast while Reid and Searcy (1986) use a Hough transform to deal with incomplete lines. A few authors make use of knowledge in addition to the fact that the lines are reasonably straight. For example Olsen (1995) scans horizontal windows in the image, sums pixel values in a vertical direction and fits sinusoidal curves to recover the periodic waveform produced by rows of equal spacing. This technique only measures the vehicle lateral offset with respect to the rows and not the vehicle angle and requires the camera to be set vertically. Gerrish and Stockman (1985) use an autocorrelation technique to make use of the periodicity in the image (i.e. several lines of equal spacing), and they also use the known optical configuration to derive a template of converging lines which can be matched with the image. Schoenfisch and Billingsley (1993) use two or three rows and make use of the known row spacing in their regression to deal with the problem of missing parts of rows.

Brivot and Marchant (1996) have shown that segmentation of plants, weeds, and soil is possible using infra-red images where the field of view is between 3 by 3 to 5 by 5 plants, i.e. of the order of 2 m square. Fig. 2a shows a typical scene containing cauliflowers. A larger field of view (i.e. a lower magnification) would not allow texture details, which are effective in differentiating plants and weeds, to be resolved. With this field of view there is little information for identifying the row structure which will be used for vehicle guidance. This means that any technique must be robust to uncertainty in the data. Uncertainty is a generic problem in analysing scenes containing biological objects (Tillett, 1991). In this case uncertainties arise from variability in planting pattern, different plant sizes, presence of weeds, image noise due to natural lighting variations, missing plants, and many other causes. One possibility is to use two cameras, one for guidance (with a wide field of view) and one for plant identification. This is a possibility but would result in extra system complexity. Also, a problem with using a wide field of view is that guidance information would be derived from an image that included the plant rows at some considerable distance from the vehicle. Although a wide field of view might seem to be an advantage in that there is more data, most of it would not be local to the vehicle and could lead to significant errors, especially if the rows are not straight. An alternative, used in this work, is to make as much use of the data and prior knowledge that is available, and to use a robust method to find the row structure in the image.

3. Basis of the row tracker

The Hough transform (Davies, 1990) is a robust method often used to find fairly simple structures in images such as straight lines or circles. As an example, imagine an image consisting of blobs and line segments lying on a straight line (Fig. 3, left). These image features could be part of a continuous line whose equation is $y = mx + c$. The two parameters of the line are the slope, m, and the intercept, c. Now consider a single feature, say the centroid of one of the blobs, labelled 1. There is a family of possible straight lines that pass through this feature point, each line having a different slope and intercept. We now plot the relationship between the slopes and the intercepts (Fig. 3, right), this is called the Hough space plot for the single feature. Now consider another

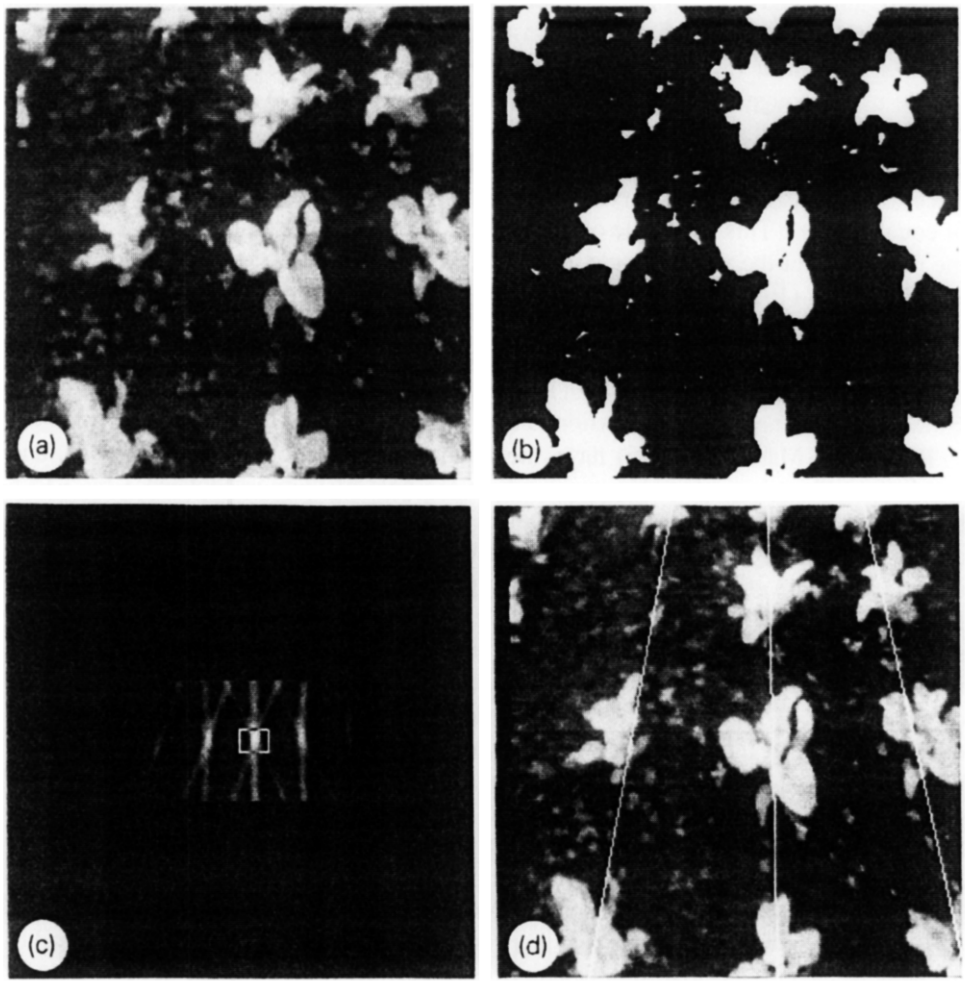

Fig. 2. Processing of cauliflower image. (a) Infra-red image; (b) thresholded; (c) Hough space; (d) identified row structure overlaid.

feature, point 2, on the image line and plot a second relationship in the Hough space. This will intersect the first one. If a third and subsequent feature are also on the image line, their Hough space plots will also intersect at the same point. This must be the case as there is only one m, c pair that will explain all the image points.

In practice the Hough space is organised as an accumulator and the plots are added into it. Thus the process can be regarded as amassing evidence for the image structure resulting in a peak building up in the accumulator. Image features that do not lie on the line (e.g. point 4) result in Hough space plots that do not support the peak. Thus the Hough transform is a type of robust estimator and can reject outliers in the data providing the number of outliers is reasonably small compared with the number of true data points. In our case the outliers are the weeds and other features, like stones, not part

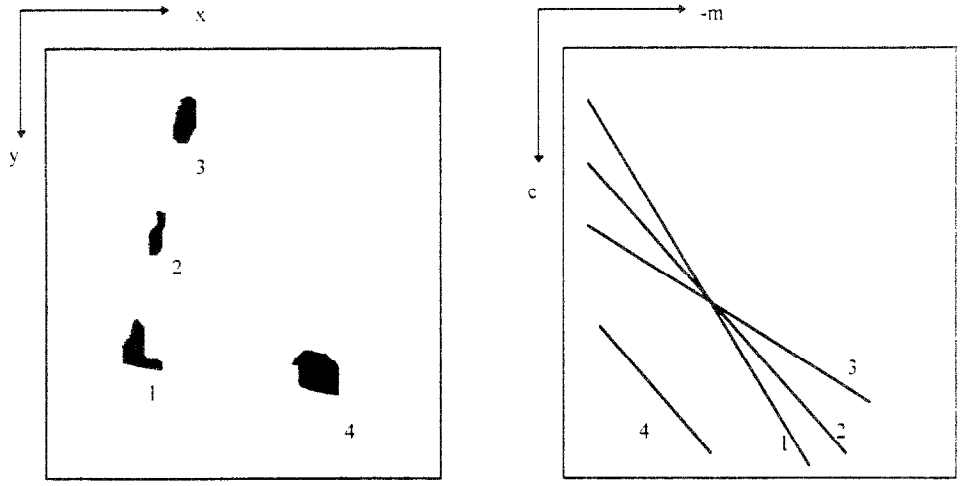

Fig. 3. Transformation from image to Hough space. Left: image features, right: plots in Hough space.

of the crop row structure. It can also deal with missing data provided there is sufficient evidence for the image structure under investigation. Thus the technique should be intrinsically tolerant to the type of image corruption we expect to find. With real data the "peak" may consist of many (hopefully close) crossing points so the Hough space has to be smoothed before being searched for a peak.

Although normally used for simple abstractions, the technique can be modified for more complex ones providing a suitable Hough space can be derived. In this work the abstraction is not a single line but a set of plant rows of constant spacing which are parallel but undergo a perspective transformation from the world to the image. This sets it apart from other work using a Hough transform to find crop rows. It means that the evidence for the row structure is integrated over each row and also over more than one row. The integration uses prior knowledge of the optics and certain fixed distances and angles (such as row spacing, and camera height and inclination), and so increases the robustness of the system compared with a technique that finds individual rows. The transform has been designed such that the axes of the Hough space are the vehicle angle and lateral offset with respect to the row structure. Hence, tracking peaks in the space will give the necessary guidance information.

The theory of a suitable Hough transform, implemented in real time at a rate sufficient to control the vehicle (10 Hz), has been presented in previous work (Marchant and Brivot, 1995). It is summarised in the Appendix for completeness. The features used to derive the curves in the Hough space are obtained by thresholding the image (Fig. 2b) and measuring the centre of the bounding box of each blob. The intensity of each line in the Hough space is weighted in accordance with the corresponding blob area. Fig. 2c shows the parameter space where five peaks can be seen, labelled 1 to 5 left to right in the following discussion. The scene contains three rows. A feature that is actually in the left row contributes to peaks 1, 2, and 3; if in the centre row peaks 2, 3, and 4 are augmented; if in the right row 3, 4, and 5 are increased. The prior geometrical

information ensures that contributions to each peak are registered correctly whatever row the feature comes from. Peak 3 is generally the highest as it contains contributions from all three rows. Note that the peak is very clear even though there is a missing plant in the leftmost row towards the top of the image. The structure projected back from the centre of this peak to the image plane is overlaid on the image in Fig. 2d.

It is quite possible (e.g. due to missing or mis-placed plants or weeds) that the "correct" peak is not the highest. This possibility is overcome by tracking the peak in Hough space rather than merely searching for it. Two techniques are used in tracking. Firstly, an approximation to the peak position is established from the vehicle controller's estimate of the movement between time steps. This estimate is derived from a fusion of the various vehicle sensors (including vision and odometry) using a Kalman filter (Hague and Tillett, 1996). Secondly, the search space around the approximate position is reduced to a small area, the size of which is established from a reasonable upper bound on the error in the estimate. The search area is shown as a rectangle in Fig. 2c. Although the search space could be allowed to change in size, a static value is used so that the time taken by the algorithm is deterministic, which is important in a real time system. Initialisation is achieved by placing the vehicle close to a central position with respect to the row structure at startup. Note that the first part of the tracking mechanism was not used in obtaining the results below as they were done off-line, i.e. the controller estimates were not available.

4. Experimental procedure

The three plant types have different planting methods and different growth habits. Cauliflower was the most regular as it was transplanted at approximately equal spacings both along and across the rows. Also, transplanting meant that the individual plants survived better so missing plants were rare. The sugar beet was less regular as it was established from seed using a brush drill after which it was hand thinned. This meant that the eventual spacing along the rows was rather irregular. The wheat had been planted as part of an investigation into the relationships between row spacing, mechanical weeding, and yield. The crop was drilled as widely spaced double rows which meant that the plants were much closer than the other two species along the rows. The spacing of row pairs was wider than conventional practice but significantly closer than the other species. The experimental data was collected at different times and with individual constraints and so the procedure was slightly different for each plant type.

4.1. Cauliflowers

The experimental field plot contained cauliflowers about 200 mm high with the rows spaced at 410 mm. The spacing along the rows was 600 mm with the camera 1200 mm above the ground. The camera was a standard CCD monochrome but enhanced in the near infra-red by removing the IR blocking filter and using a bandpass filter to remove visible wavelengths. The camera angle to the vertical and the effective focal length were calibrated (Marchant and Brivot, 1996) to be 64° and 37 mm, respectively. Data was first recorded onto video tape in mixed illumination conditions and then digitised into

images of 256 × 256 pixels. The total length of the video recording was about 6 min during which the vehicle speed varied between 0.3 and 0.6 m s^{-1}. The vehicle was driven manually. Three sections of tape were selected for digitising where the driver made large, approximately sinusoidal, deviations from the forward path. Two sequences from each section were digitised into 30 images each, giving a total of 180 images. As the vehicle speed was rather slow (it is difficult to drive the vehicle in this way at high speeds) and variable, the digitization rate was adjusted to grab images at a rate equivalent to 10 Hz at 2 m s^{-1} speed (i.e. every 200 mm of travel).

4.2. Sugar beet

The sugar beet was established in rows spaced at 450 mm. The spacing along the rows was approximately 150 mm and the plants were about 120 mm high. The camera height was 1400 mm. The camera angle and the effective focal length were 30° and 23 mm, respectively. The speed was 0.3 m s^{-1} and the images were grabbed directly onto disc at intervals of 500 ms in uniform overcast conditions. Six sequences were grabbed, most of them with the vehicle driven in a reasonably straight line.

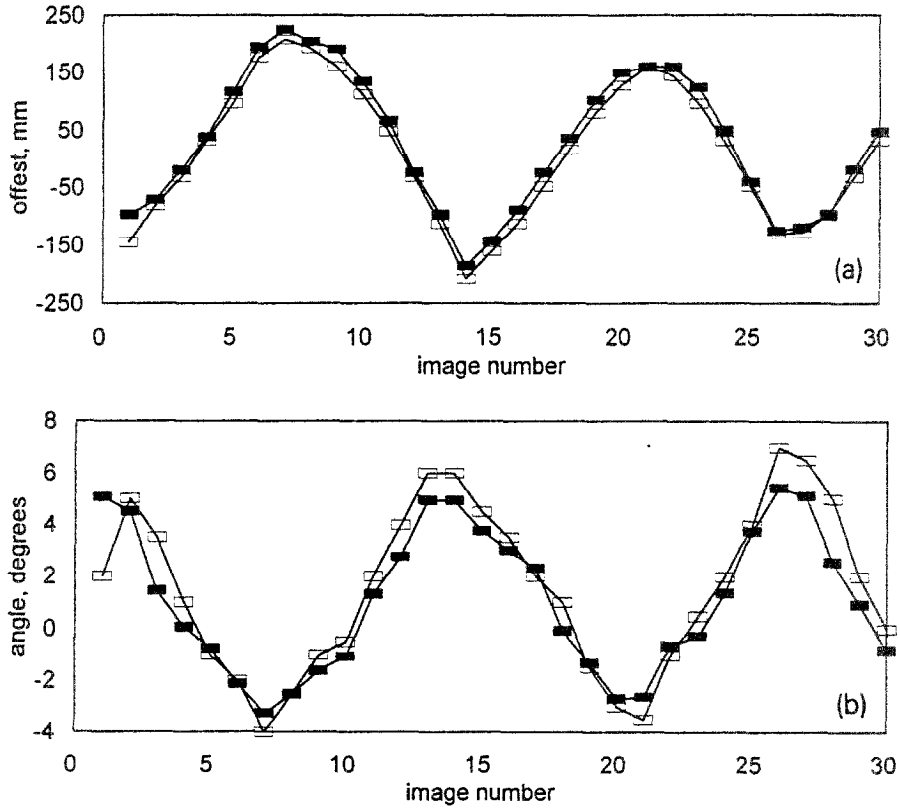

Fig. 4. Typical result for cauliflower. (a) Offset; (b) angle. □ = automatic: ■ = manual.

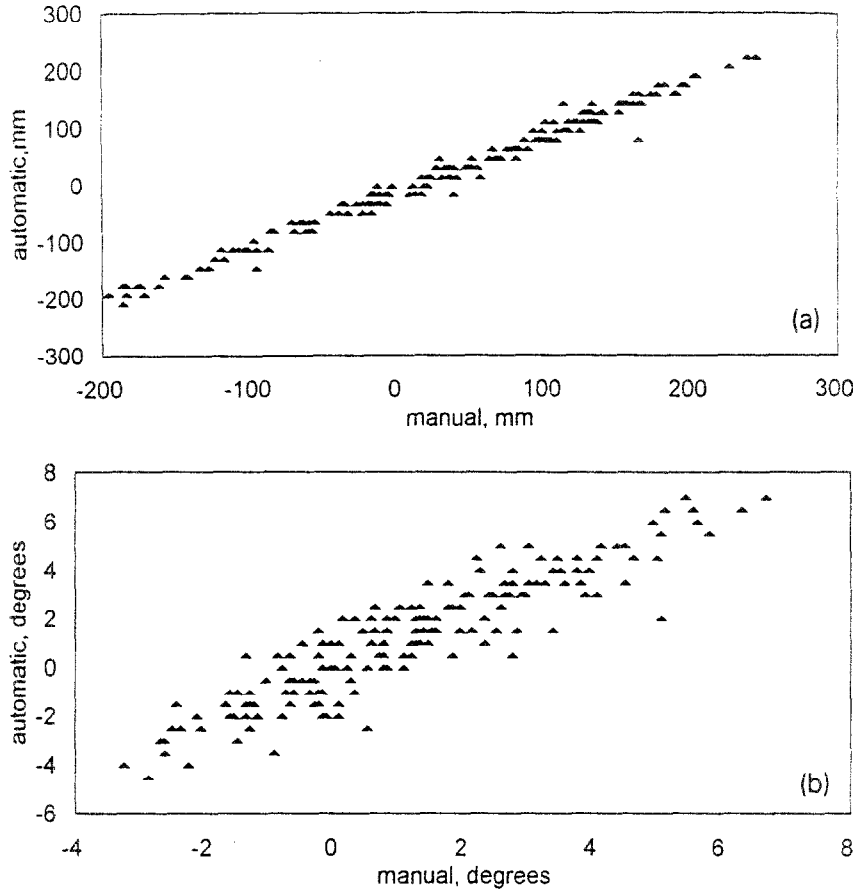

Fig. 5. Automatic vs. manual measurement for cauliflower. (a) Offset; (b) angle.

4.3. Wheat

Data were collected in bright sunshine from plots of winter sown wheat in double rows. Visually this appeared as dense bands of vegetation (the double rows) with gaps between them. The effective row spacing between the bands was 350 mm. Growth stage was 2–3 tillers with an approximate height of 50 mm.

Some difficulty was experienced with the timing of the experiments. The original intention was to mount the camera on a vehicle to give a uniform camera height and angle. However, the previous period had been very wet and taking a vehicle onto these experimental plots was inadvisable. Consequently an alternative approach was adopted. A hand-held rig was constructed consisting of a horizontal boom about 6 m long with a drop-arm clamped at right angles to the middle. The boom was carried at shoulder height by an operator at each end and a weight on the end of the drop-arm acted as a pendulum and kept the arm approximately vertical. The camera was attached via a pan/tilt head to the drop-arm and so maintained an approximately constant attitude. A

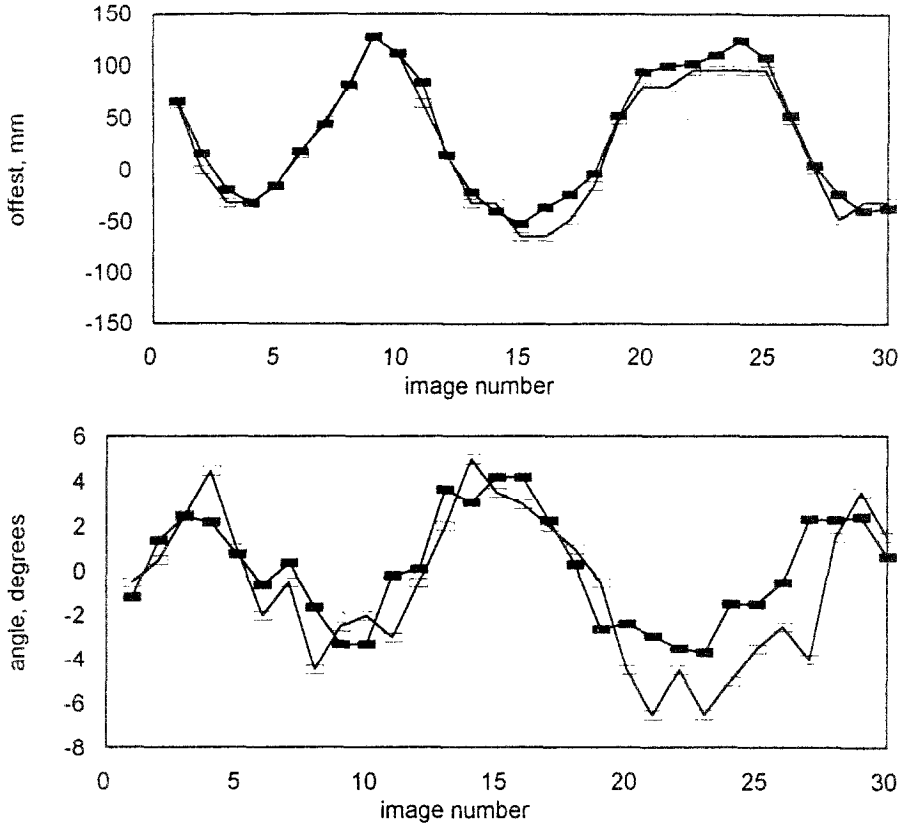

Fig. 6. Typical result for sugar beet. (a) Offset; (b) angle. □ = automatic; ■ = manual.

third operator walked behind with a video recorder. The forward speed was about 1 m s^{-1} and 30 images were digitised in the laboratory from each run at a rate of one every 140 ms. The camera height was 1130 mm, the angle to the vertical 56°, and the effective lens focal length was 19 mm.

Four runs were carried out. Two where the operators walked an approximately straight course and two where the operators imparted an approximately sinusoidal variation to the boom horizontal angle to simulate a variable heading. They did this by one operator keeping a constant speed while the other alternately speeded up and slowed down. The first of these runs was with the sun behind and the second with the sun ahead.

Strictly, all of the requirements of the theory (horizontal planar ground, straight parallel rows, constant row spacing, constant camera height, constant camera pitch angle, zero roll angle) were violated. In practice most were violated only as they would be by normal growing and field conditions. In addition there were shadows from the equipment and the operators. There was yet another problem caused by the hand-held rig. Normal walking imparted a vertical undulation and a swinging motion to the pendulum and so the camera changed its viewpoint during the runs. This problem was worse in the sinusoidal runs. In these cases it was more difficult to concentrate on the two problems

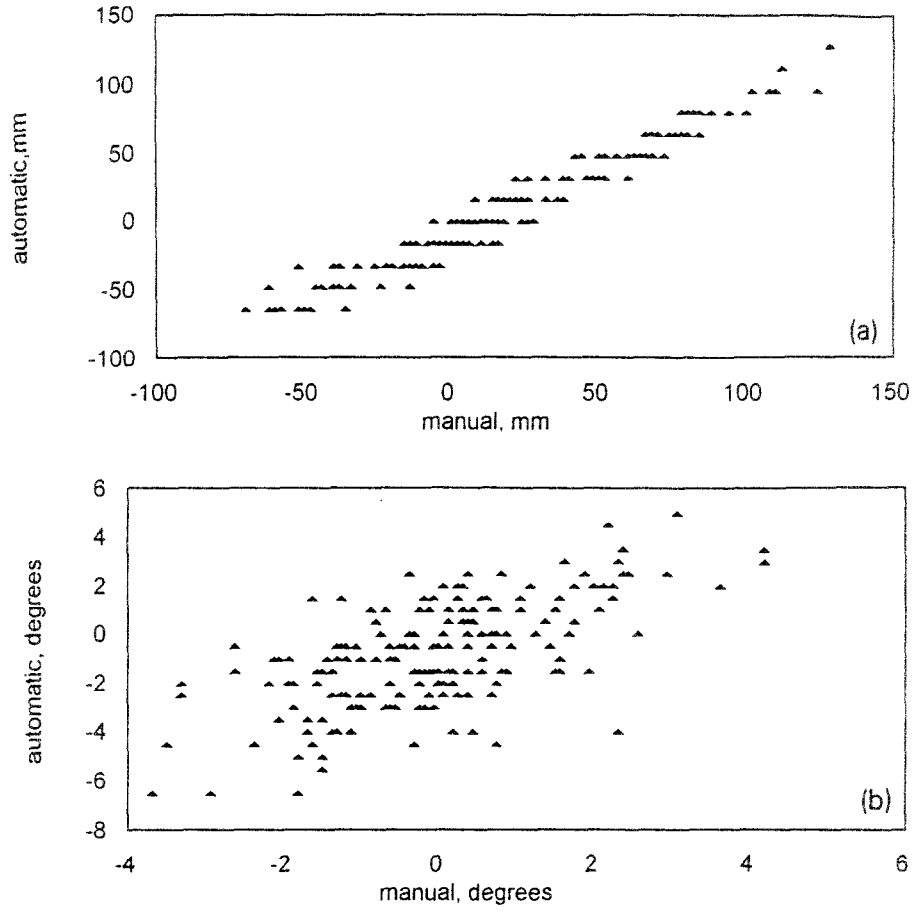

Fig. 7. Automatic vs. manual measurement for sugar beet. (a) Offset; (b) angle.

of producing a sinusoidal path while keeping the boom steady. However, although the camera motion was not quite ideal, the deficiencies provided a good test of the robustness of the algorithm which, after all, must cope with normal operational variations.

Two modifications were made to the original algorithm. The first one arises because of the different growth habit and planting regime of cereals compared with transplanted vegetables. This causes the plants to merge along the rows rather than forming discrete blobs in the image. Four black horizontal lines were drawn in each image at equal distances apart so dividing the images into horizontal bands and splitting the rows into separate blobs. The second modification arose from the shallower angle of the camera. This meant that the field of view was longer and included more plants further from the camera. If rows are not straight (as is likely in practice) then including these plants could give false estimates. A more sensible course of action is to weight the near plants more highly compared with the distant ones as the Hough space is loaded. This means that the estimates are biased towards the near plants which are the important ones when

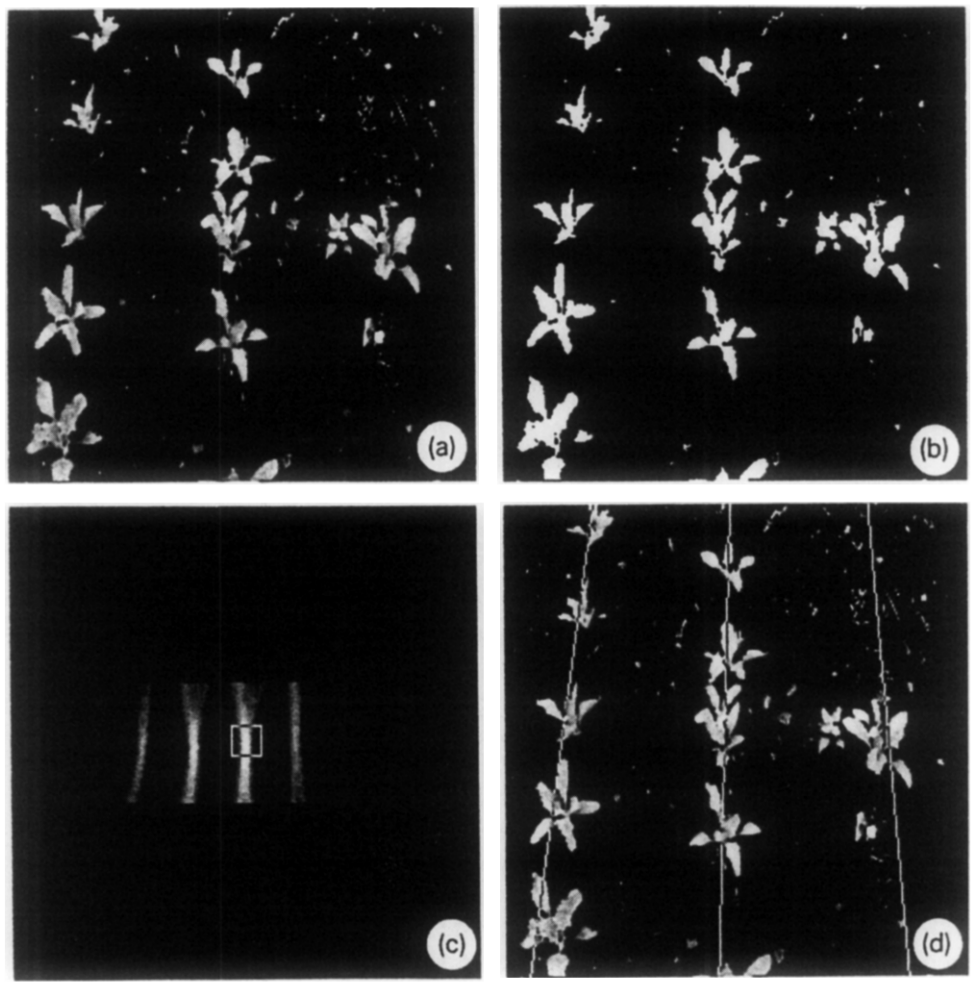

Fig. 8. Processing of sugar beet image. (a) Infra-red image; (b) thresholded; (c) Hough space; (d) identified row structure overlaid.

applying a treatment. This was achieved simply by multiplying the contribution to the Hough space by the distance from the top of the image to the feature.

4.4. Method of analysis

To measure the accuracy of the offset and heading angle, the output was compared with a human assessment of the images. However, establishing "ground truth" by this method is problematical. As the plants are natural objects and planted in a natural medium there is some subjectivity about their "position". A program was written to display each image and to allow an operator to control the position of an overlaid plant row structure with a mouse. The two mouse axes controlled the offset and angle

assuming the camera optics and position were as established above. The result was hidden from the operator until the end of the run to avoid his estimates being influenced by the tracker output. The measurements for both automatic and manual methods were done to finite resolutions. These were 16 mm (offset) and 1° (angle) for automatic and 2 mm and 0.062° for the manual method. This finite resolution can add slightly to any discrepancy between the two methods. The objective of this work is to assess the accuracy of the row tracker only and so a comparison between the row structure positions in the images is appropriate. Errors in control caused by calibration between image and ground coordinates and by the controller performance are not included here. This would be tested by comparing the controlled vehicle position with respect to the row structure on the ground and will be reported in a later paper.

5. Results

5.1. Cauliflowers

Fig. 4 shows plots of offset and angle for a typical sequence. Visually, the automatic measurements track the human assessments reasonably well. The approximately sinusoidal path followed by the vehicle driver can be clearly seen. To determine the statistical relationships between the two methods, automatic and human measurements were plotted against one another in Fig. 5. The plots include all the measurements from all six runs. Although measurement errors could have come from either human or automatic methods, all the errors were assumed to be in the automatic ones. This should give an upper bound to the error estimates.

A linear regression was performed for offset and angle, the statistics are shown in Table 1. The reason for the non-zero intercept of the offset is not clear, however its magnitude (approx. 10 mm) is small enough to be neglected. The reason for the slopes being different from 1.0 is also not clear. However, any feedback controller will aim to bring both offset and angle to zero in the steady state, thus values slightly different from 1.0 will affect only the dynamic response and even then only slightly. Any adverse effect will be removed by slightly re-tuning the controller.

A measure of the typical errors in measurement can be obtained from the r.m.s. deviation of the data from the fitted regression lines. For the offset this is 12.5 mm and

Table 1
Statistics of the results for the three crops

Crop	Offset (mm)			Angle (degrees)		
	a	b	c	a	b	c
Cauliflower	0.96 to 0.99	−12.2 to −8.3	12.5	1.01 to 1.15	−0.17 to 0.17	1.0
Sugar beet	0.94 to 1.01	−11.8 to −8.7	9.8	0.78 to 1.12	−0.97 to −0.47	1.7
Wheat	0.98 to 1.01	−10.2 to −1.4	17.7	0.93 to 1.01	−0.14 to 0.36	0.9

a = 95% confidence limits for the slope of the regression line.
b = 95% confidence limits for the intercept of the regression line.
c = r.m.s. deviation of the measurements from the regression line.

for the angle 1.0°. Neither of these values is expected to prove a problem in vehicle control, especially as the effect of vision errors will be reduced when the data are fused with odometry in the vehicle controller (Hague and Tillett, 1996).

5.2. Sugar beet

Figs. 6 and 7 show a typical result for sugar beet with the statistics for all six runs given in Table 1. Once again the tracking appears to be good, especially for the offset. There is a noticeable reduction in agreement for the angle compared with the cauliflower runs which is also shown in an increased angle error (1.7°) in Table 1. One cause of this can be seen from Fig. 8c where the Hough space is shown. Note that the individual lines cross at a shallower angle compared with the case for cauliflower (Fig. 2c), making the peak less focussed along the angle (vertical) axis. It can be shown that the crossing angle is greater when the field of view covers more distance along the crop rows. One way of achieving this is to use a camera more inclined to the vertical, which was the case of the cauliflower runs compared with those for the sugar beet.

Fig. 8 has been chosen to illustrate a situation with a number of missing plants along with some weed contamination. The peaks in the Hough space are still clear and the measured row position still agrees with a human assessment. Note that the rightmost line in the Hough space is very weak as it is supported by only one plant blob in the right-hand row.

5.3. Wheat

The wheat crop situation is shown in Fig. 9 where a typical tracking result is overlaid on an infra-red image. Note the twin row layout which is apparent in the identified

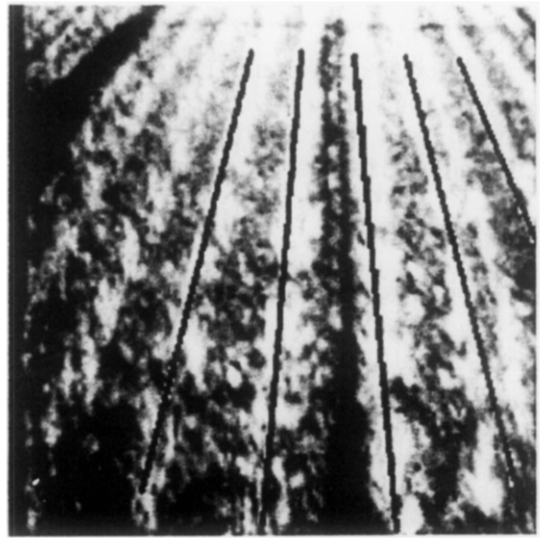

Fig. 9. Typical result for wheat showing identified row structure overlaid on infra-red image.

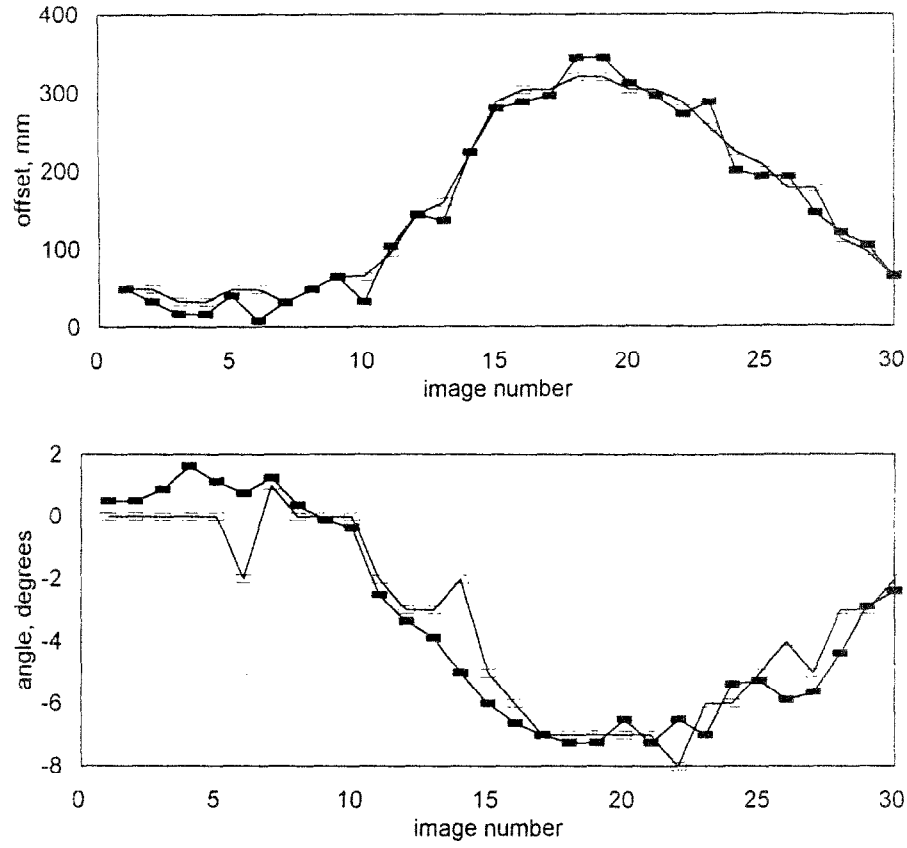

Fig. 10. Typical result for wheat. (a) Offset; (b) angle. □ = automatic; ■ = manual.

row second from the right. Results are shown in Figs. 10 and 11 and Table 1. One of the approximately sinusoidal paths is shown although less than a complete cycle was completed due to the limited length of the experimental plots. Agreement is again good with typical errors of 17.7 mm of offset and 0.9° of angle.

6. Conclusions

It is possible to derive a Hough transform which integrates information over a number of plant rows given the row spacing, the camera calibration, and the camera position. Thresholded plant blobs are used as input features. The Hough transform can be used to find the vehicle offset and heading angle with respect to the plant rows. Algorithms developed in other work for individual plant discrimination require a close-up view providing comparatively few features for the transform. Integration over rows, as well as within rows, provides the robustness to allow operation with few features. The algorithm worked well when tested on a number of sequences of 30 images of three crops; cauliflower, sugar beet, and wheat grown in widely spaced rows. Typical errors

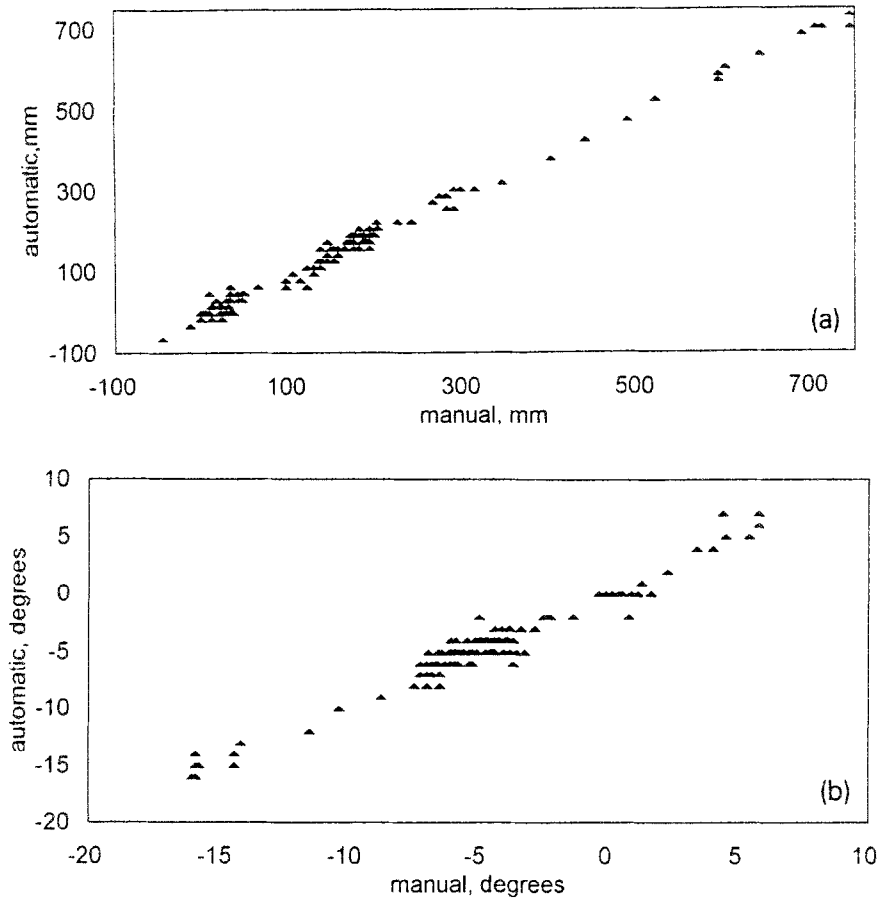

Fig. 11. Automatic vs. manual measurement for wheat. (a) Offset; (b) angle.

were less than 18 mm of offset and, with the exception of the beet runs, less than 1.0° of angle. The angular accuracy for beet could probably be improved by adjusting the optical configuration to give more perspective.

In current work the method has been implemented in a real time system and the vision data fused with odometry and other data in the vehicle controller. Experience with the vehicle (to be reported in due course) suggests that the accuracies are adequate for control purposes.

Acknowledgements

This work presents results from two projects at SRI. The first is funded by the Biotechnology and Biological Sciences Research Council under the Clean Technology Programme. The second was funded by the Ministry of Agriculture, Fisheries, and Food. Thanks are due to Alister Blair of the ADAS Boxworth Research Centre for permission to endanger his experimental plots of winter wheat.

Appendix

Fig. 12 shows the geometry of the coordinate systems. The heading angle, Ψ, and the offset, h need to be found in order to control the vehicle. It is assumed that the ground is flat; the camera angle, ϕ, and its height above the ground, v, are constant; and the camera optics can be represented by a pin hole model. In order to keep the dimensionality of the Hough space down to two, it is further assumed that the vehicle

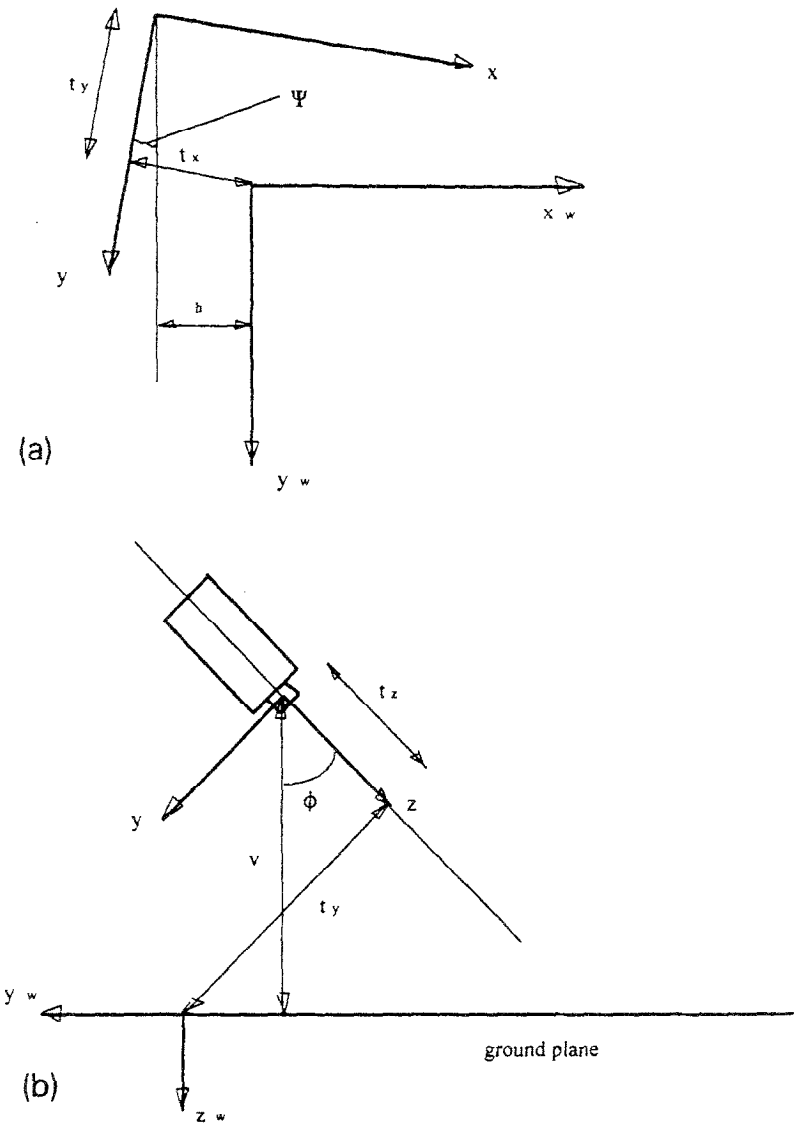

Fig. 12. Geometry of coordinate systems. (a) Plan view; (b) side view.

does not roll or pitch. The only rotation assumed is yaw which produces the vehicle heading angle. The justification for these assumptions is that the ground in a prepared horticultural seedbed will be fairly flat. Errors caused by these assumptions will be reflected in inaccuracies in the determined heading angle and offset.

Tsai (1986) gives relationships between the various coordinate systems. In general

$$\begin{bmatrix} x \\ y \\ z \end{bmatrix} = \begin{bmatrix} r_1 & r_2 & r_3 \\ r_4 & r_5 & r_6 \\ r_7 & r_8 & r_9 \end{bmatrix} \begin{bmatrix} x_w \\ y_w \\ z_w \end{bmatrix} + \begin{bmatrix} t_x \\ t_y \\ t_z \end{bmatrix} \tag{1}$$

If we assume pitch = roll = 0, then $r_1 = \cos(\Psi)$, $r_2 = \sin(\Psi)$, $r_3 = 0$, $r_4 = -\sin(\Psi)\cos(\Phi)$, $r_5 = \cos(\Psi)\cos(\Phi)$, $r_6 = \sin(\Phi)$, $r_7 = \sin(\Psi)\sin(\Phi)$, $r_8 = -\cos(\Psi)\sin(\Phi)$, and $r_9 = \cos(\Phi)$.

The pin hole camera model results in

$$x_u = \frac{f}{z}x \qquad y_u = \frac{f}{z}y \tag{2}$$

where x_u, y_u, are the positions in the image plane corresponding to x, y, and f is the effective focal length of the camera (i.e. the distance of the image plane from the origin of the camera coordinate system).

We now use Eq. 2 and Tsai's notation for the elements of $[R]$ to obtain

$$x_u = f\frac{(r_1x_w + r_2y_w + t_x)}{r_7x_w + r_8y_w + t_z} \qquad y_u = f\frac{(r_4x_w + r_5y_w + t_y)}{r_7x_w + r_8y_w + t_z} \tag{3}$$

Without loss of generality we can assume $t_y = 0$, i.e. the x_w axis passes through the point where the camera axis intersects the ground. Also, as the plants are in equally spaced rows parallel to the y_w axis and the y_w axis is assumed to coincide with a plant row, then for any plant $x_w = nr$ where r is the row spacing and n is a whole number. We also assume that Ψ is small and so $\cos(\Psi) = 1$ and $\sin(\Psi) = \Psi$.

Using the above assumptions we obtain from Eq. 3

$$y_w(-Sx_u - f\psi) = -x_u(S\psi nr + t_z) + f(nr + t_x) \qquad y_w(-Sy_u - fC) = -y_u(S\psi nr + t_z) + f(-C\psi nr) \tag{4}$$

where $S = \sin(\phi)$ and $C = cos(\phi)$. Eliminating y_w and simplifying gives

$$A\psi^2 + D\psi + Et_x + Fnr + G = 0 \tag{5}$$

where $A = nr(y_uS + fC)$; $D = y_ut_z$; $E = Sy_u + Cf$; $F = E$; $G = -x_uCt_z$. From Fig. 12, $t_z = v/\cos(\phi)$. Also, with $t_y = 0$ and small ψ, $h = t_x$.

If we measure the position of any feature in the image plane x_u, y_u, the only unknowns in Eq. 5 are ψ and t_x (the heading angle and offset position, i.e. the parameters required for vehicle control) and n.

To calculate feature positions in the image plane we use the following results from Tsai

$$\begin{aligned} x_u &= (x_f - C_x)\mathrm{d}x \\ y_u &= (y_f - C_y)\mathrm{d}y \end{aligned} \tag{6}$$

This assumes no lens distortion. C_x and C_y are the coordinates of the optical centre of the camera in pixels and so are set to half the image size, i.e. 128. dx and dy are the sizes of the sensor elements in the x and y directions. Their values are unimportant as they merely provide an arbitrary scaling for x_u, y_u, and f. Details of how to calibrate for f, ϕ, and an initial value for t_x are found in Marchant and Brivot (1996).

Given the position of a feature (say the centre of a plant blob) in the image, Eq. 5 gives values from all possible combinations of ψ and t_x that could have produced that feature position. Thus the two-dimensional plane of ψ vs. t_x can be regarded as a Hough space with Eq. 5 allowing us to map feature point positions to curves in the space. In normal applications of the Hough Transform, a feature position generates a single curve in Hough space. The images used in this work contain about three or four rows of plants and so we consider that each feature could have come from any of three rows. Thus each feature generates three curves in the Hough space i.e. by using Eq. 5 with n set to -1, 0, or $+1$.

References

Brandon, J.R., Searcy, S.W. and Babowicz, R.J. (1989) Distributed control for vision based tractor guidance. ASAE Paper 89-7517.

Brivot, R. and Marchant, J.A. (1996) Segmentation of plants and weeds using infrared images. Acta Hortic. (in press).

Brown, N.H., Wood, H.C. and Wilson, J.N. (1990) Image analysis for vision based agricultural vehicle guidance. Proc. SPIE Conf. Optics in Agriculture, Boston, pp. 54–68.

Davies, E.R. (1990) Machine Vision: Theory, Algorithms, Practicalities. Academic Press, London.

Derras, M., Berducat, M. and Bonton, P. (1991) Vision guided mower for the upkeep of natural environment. Proc. 1st Int. Seminar On Machine Vision Systems for the Agricultural and Bio-Industries, Montpellier, pp. 37–46.

Fehr, B.W. and Gerrish, J.B. (1989) Vision guided off-road vehicle. ASAE Paper 89-7516.

Hague, T. and Tillett, N.D. (1996) Navigation and control of an autonomous horticultural robot. Mechatronics, 6(2): 165–180.

Gerrish, J.B. and Stockman, G.C. (1985) Image processing for path finding in agricultural field operations. ASAE Paper 85-3037.

Marchant, J.A. and Brivot, R. (1995) Real time tracking of plant rows using a Hough transform. Real Time Imaging, 1: 363–375.

Olsen, H.J. (1995) Determination of row position in small-grain crops by analysis of video images. Comput. Electron. Agric., 12: 147–162.

Reid, J.F. and Searcy, S.W. (1986) Detecting crop rows using the Hough transform. ASAE Paper 86-3042.

Schoenfisch, M. and Billingsley, J. (1993) A comparison of automated guidance systems for a variety of operations in the growing of cotton. Proc. 3rd Int. Workshop IARP, Brisbane, pp. 8–16.

Stafford, J.V. and Ambler, B. (1994) In-field location using GPS for spatially variable field operations. Comput. Electron. Agric., 11: 23–26.

Tillett, R.D. (1991) Image analysis for agricultural processes: a review of potential opportunities. J. Agric. Eng. Res., 50: 247–258.

Tsai, R.Y. (1986) An efficient and accurate camera calibration technique for 3D machine vision. Proc. IEEE Computer Soc. Conf. Computer Vision and Pattern Recognition, Miami Beach.